



**HAL**  
open science

## Common and Exclusive Features of Intestinal Intraepithelial $\gamma\delta$ T Cells and Other $\gamma\delta$ T Cell Subsets

Apostol Apostolov, Miriame Hamani, Hector Hernandez-Vargas, Ramdane Igalouzene, Alexandre Guyennon, Olivier Fesneau, Julien Marie, Saidi Soudja

### ► To cite this version:

Apostol Apostolov, Miriame Hamani, Hector Hernandez-Vargas, Ramdane Igalouzene, Alexandre Guyennon, et al.. Common and Exclusive Features of Intestinal Intraepithelial  $\gamma\delta$  T Cells and Other  $\gamma\delta$  T Cell Subsets. *ImmunoHorizons* , 2022, 6 (7), pp.515-527. 10.4049/immunohorizons.2200046 . hal-03848188

**HAL Id: hal-03848188**

**<https://hal.science/hal-03848188v1>**

Submitted on 21 Nov 2023

**HAL** is a multi-disciplinary open access archive for the deposit and dissemination of scientific research documents, whether they are published or not. The documents may come from teaching and research institutions in France or abroad, or from public or private research centers.

L'archive ouverte pluridisciplinaire **HAL**, est destinée au dépôt et à la diffusion de documents scientifiques de niveau recherche, publiés ou non, émanant des établissements d'enseignement et de recherche français ou étrangers, des laboratoires publics ou privés.



**ImmunoHorizons**  
**CALL FOR IMMUNOLOGY EDUCATION PAPERS!**  
Visit [ImmunoHorizons.org](https://www.immunohorizons.org) for more information!



RESEARCH ARTICLE | JULY 01 2022

## Common and Exclusive Features of Intestinal Intraepithelial $\gamma\delta$ T Cells and Other $\gamma\delta$ T Cell Subsets

Apostol K. Apostolov; ... et. al

*Immunohorizons* (2022) 6 (7): 515–527.

<https://doi.org/10.4049/immunohorizons.2200046>

### Related Content

Intra- and Intercompartmental Movement of  $\gamma\delta$  T Cells: Intestinal Intraepithelial and Peripheral  $\gamma\delta$  T Cells Represent Exclusive Nonoverlapping Populations with Distinct Migration Characteristics

*J Immunol* (November,2010)

Differential Effects of IL-2 and IL-15 on the Death and Survival of Activated TCR $\gamma\delta^+$  Intestinal Intraepithelial Lymphocytes

*J Immunol* (February,1999)

Lymphoid Hyperplasia, Autoimmunity, and Compromised Intestinal Intraepithelial Lymphocyte Development in Colitis-Free Gnotobiotic IL-2-Deficient Mice

*J Immunol* (January,1998)

# Common and Exclusive Features of Intestinal Intraepithelial $\gamma\delta$ T Cells and Other $\gamma\delta$ T Cell Subsets

Apostol K. Apostolov,<sup>1</sup> Miriame Hamani,<sup>1</sup> Hector Hernandez-Vargas, Ramdane Igalouzene, Alexandre Guyennon, Olivier Fesneau, Julien C. Marie, and Saïdi M'homa Soudja

Tumor Escape Resistance Immunity Department, Cancer Research Center of Lyon, UMR INSERM 1052, CNRS 5286, Université Claude Bernard Lyon 1, Centre Léon Bérard, Lyon, France

## ABSTRACT

Murine peripheral lymph node TCR  $\gamma\delta$  T cells have been divided into type 1 and type 17 functional categories based on phenotypic and functional markers. Localized in the gut epithelial barrier, intestinal intraepithelial lymphocytes (iIEL)  $\gamma\delta$  T cells constitute a peculiar subset of T lymphocytes involved in intestinal homeostasis. However, whether iIEL  $\gamma\delta$  T cells obey the type 1/type 17 dichotomy is unclear. Using both global transcriptional signatures and expression of cell surface markers, we reveal that murine iIEL  $\gamma\delta$  T cells compose a distinct population, expressing ~1000 specific genes, in particular genes that are responsible for cytotoxicity and regulatory functions. The expression of the transcription factor Helios is a feature of iIEL  $\gamma\delta$  T cells, distinguishing them from the other TCR  $\gamma\delta$  T subsets, including those present in the epithelia of other tissues. The marked expression of Helios is also shared by the other iIELs, TCR $\alpha\beta$ CD8 $\alpha\alpha$  lymphocytes present within the intestinal epithelium. Finally, we show that Helios expression depends in part on TGF- $\beta$  signaling but not on the microbiota. Thus, our study proposes iIEL  $\gamma\delta$  T cells as a distinct subset and identifies novel markers to differentiate them from their peripheral counterparts. *ImmunoHorizons*, 2022, 6: 515–527.

## INTRODUCTION

The intestinal epithelium represents the largest barrier surface separating the host from the external environment. It consists of a physical and chemical barrier adapted to food contact and commensal bacterial colonization (1). The local presence of immune cells is of crucial importance in this microbe-enriched environment. The close collaboration between epithelial and immune cells maintains epithelial integrity and immune homeostasis (2). A large

number of the immune cells in the gut are represented by intestinal intraepithelial lymphocytes (iIELs), which have intimate contact with intestinal epithelial cells (3). Two categories of iIELs have been classified, induced and natural. The induced iIELs derive from conventional, naive-like CD8 $\alpha\beta^+$  T cells or CD4 $^+$  T cells, bearing a conventional TCR formed by  $\alpha$ - and  $\beta$ -chains. After their thymus egress and differentiation into effector cells, a fraction of conventional T cells migrate to the gut and give rise to induced iIELs (4). An “alternative”

Received for publication May 27, 2022. Accepted for publication June 25, 2022.

**Address correspondence and reprint requests to:** Dr. Saïdi M'homa Soudja, Cancer Research Center of Lyon, 28 rue Laennec, Cheney B, 4<sup>ème</sup> Étage, 69008 Lyon, France. E-mail address: saïdi.soudja@inserm.fr

ORCIDiDs: 0000-0002-8825-582X (A.K.A.); 0000-0002-7961-6021 (M.H.); 0000-0002-4226-0471 (O.F.).

<sup>1</sup>A.K.A. and M.H. contributed equally to this work.

The sequencing data presented in this article have been submitted to the Gene Expression Omnibus under accession number GSE198703.

This work was supported by Fondation ARC pour la Recherche sur le Cancer Grant PJA 20151203509- ARCD0C42020070002550 (to S.M.S. and R.I.), the French Ministry of Research (to R.I.), and by LabEx DEVweCan ANR Investissement d'Avenir (to J.C.M.).

M.H., A.K.A., A.G., O.F., and R.I. performed experiments. H.H.-V. performed the bioinformatics analysis. M.H., A.K.A., H.H.-V., and S.M.S. analyzed experiments. A.K.A., M.H., H.H.-V., S.M.S., and J.C.M. discussed the data and provided conceptual input. S.M.S. and J.C.M. provided financial resources. A.K.A. and S.M.S. wrote the manuscript.

**Abbreviations used in this article:** iIEL, intestinal intraepithelial lymphocyte; LAP, latency-associated protein; PCA, principal component analysis; pLN, peripheral lymph node; SI, small intestine; T1, type 1; T17, type 17; Tn, naive-like T; Treg, regulatory T cell.

The online version of this article contains supplemental material.

This article is distributed under the terms of the [CC BY 4.0 Unported license](https://creativecommons.org/licenses/by/4.0/).

Copyright © 2022 The Authors

<https://doi.org/10.4049/immunohorizons.2200046>

*ImmunoHorizons* is published by The American Association of Immunologists, Inc.

thymic selection leads to the generation of natural iIELs that bear either a TCR $\alpha\beta$  corresponding to CD8 $\alpha\alpha^+$  TCR $\alpha\beta$  T cells or a  $\gamma\delta$  TCR corresponding to the TCR  $\gamma\delta$  T cells (5). Upon successful thymic selection and maturation, the natural TCR  $\gamma\delta$  iIELs are guided to different barrier surfaces, including the skin, lungs, urogenital tract, and gut in response to chemokines (6). Specific tissue localization and interaction with defined ligands shape the differentiation of the different  $\gamma\delta$  T cell subsets. Expression of the Skint-1 ligand by keratinocytes allows the maintenance and the differentiation of dendritic epidermal TCR  $\gamma\delta$  T cells in the skin (7), and the expression of butyrophilin-like molecules by intestinal epithelial cells allows the differentiation and maturation of iIEL TCR  $\gamma\delta$  T cells within the intestine (8).

In mice, the largest part of iIELs corresponds to  $\gamma\delta$  T cells, which may constitute 50–60% of small intestine (SI) iIELs (9). It has been suggested that  $\gamma\delta$  T iIELs ensure the homeostasis of the gut epithelium by secreting epithelial growth factors, such as keratinocyte growth factor (KGF), or cytokines essential for epithelial integrity (10). Moreover, by secreting antimicrobial peptides, the  $\gamma\delta$  T iIELs could contribute to the restriction of pathological microbial invasion (11).

Functionally two distinct subsets of  $\gamma\delta$  T cells have been defined based on their cytokine secretion profile and surface marker expression. The type 1 (T1)  $\gamma\delta$  T cells, expressing the transcription factor T-bet and the costimulatory molecule CD27, secrete IFN- $\gamma$ , and the type 17 (T17)  $\gamma\delta$  T cells, which express the transcription factor ROR $\gamma$ t, but not CD27, secrete IL-17 (12). However, whether the T1/T17 dichotomy can be transferred to iIEL  $\gamma\delta$  T cells remains elusive. The iIEL  $\gamma\delta$  T cells have been transcriptionally characterized (13–15), but information regarding transcription factors that govern their functions is still missing and the transcriptional comparison with different specific subsets of TCR  $\gamma\delta$  T cells is largely unexplored.

To get insight into the molecular features and markers of iIEL  $\gamma\delta$  T cells, we analyzed their phenotype by in-depth comparison with well-described  $\gamma\delta$  T cell subsets present in other tissues. We demonstrated that iIEL  $\gamma\delta$  T cells are phenotypically distinct from T1 cells, T17 cells, and the recently described peripheral CD44<sup>low/-</sup>CD27<sup>+</sup>  $\gamma\delta$  T cell population (16) by a side-by-side comparison. We identified markers that help to distinguish them, among which Helios expression is predominantly associated with natural iIELs compared with the induced iIELs at a steady state and largely influenced by TGF- $\beta$  signaling. Hence, this study suggests a new functional classification for iIEL  $\gamma\delta$  T cells.

## MATERIALS AND METHODS

### Mice

Males and females, of C57BL/6 genetic background mice, were used in this study. TGF- $\beta$ 2 knockout mice were obtained as described (17). Mice were maintained in a specific pathogen-free animal facility (AniCan, Centre Léon Bérard, Lyon, France). Mice were handled in accordance with institutional guidelines.

### Antibiotic treatment since in utero life

For antibiotic treatment, drinking water was supplemented with an antibiotic mixture composed of ampicillin (1 g/l), metronidazole (1 g/l), neomycin (1 g/l), and vancomycin (0.5 g/l), all purchased from Sigma-Aldrich. Breeding of wild-type mice was set up and put under either antibiotics or water. The offspring were left under antibiotics for 3 mo before the experiment.

### Cell isolation

Gut content was flushed out with PBS. For the SI, Peyer's patches were removed. Colon and SI were opened and cut into pieces of 0.5 cm and incubated for 20 min at 37°C under agitation in HBSS (Life Technologies) containing 1 mM DTT, 5 mM EDTA, 10 mM HEPES, and 5% FBS (Life Technologies). For the skin cells, ears were crushed and digested for 60 min at 37°C under agitation in complete RPMI 1640 media containing 10% FBS, 1% HEPES (Life Technologies) 1% penicillin/streptomycin (Life Technologies), 1% L-glutamine (Invitrogen/Life Technologies), collagenase (100 mg/ml; Sigma-Aldrich), and DNase I (10 mg/ml; Roche). After incubation, supernatants were filtered through nylon mesh, pelleted, and resuspended in 40% Percoll (GE Healthcare). This cell suspension was overlaid with 70% Percoll and centrifuged at 1300  $\times$  g for 20 min without break. iIELs were recovered from the interphase. Peripheral lymph nodes (pLNs) (axillary, brachial, and inguinal LNs), mesenteric lymph nodes, spleen, and Peyer's patches were mashed and filtered to obtain a single-cell suspension. For the spleen, RBCs were removed by incubating in lysis buffer (0.9% NH<sub>4</sub>Cl). Livers were mashed, filtered, and subjected to the Percoll gradient centrifugation identically to as for the intestine and the ears.

### Flow cytometry analysis

The cells were stained with the following Abs: CD45 (BD Pharmingen, clone 30-F11), CD3 (BD Pharmingen, clone RM4-5), CD4 (BD Horizon, clone RM-4-5), CD8 (eBioscience, clone 53-6,7), CD5 (BD Biosciences, 53-7.3), CD39 (eBioscience, 24DMS1), CD73 (eBioscience, eBioTY/11.8), CXCR3 (eBioscience, CXCR3-173), CCR6 (BioLegend, 29-2L17), CTLA4 (BD Biosciences, UC10-4F10-11), PD-1 (eBioscience, RMP1-30), latency-associated protein (LAP; eBioscience, TW7-16B4), TIGIT (eBioscience, GIGD7), NK1.1 (BD Pharmingen, clone PK136), TCR $\beta$  (BD Biosciences, H57-597), CD44 (eBioscience, IM7), CD27 (BD Bioscience, LG2A10), CD103 (eBioscience, 2E7), 2B4 (eBioscience, eBio244F4), and TCR $\gamma\delta$  (BD Pharmingen, clone GL3) in 1 $\times$  PBS, FCS, 1% azide. For intracellular staining, cells were fixed and permeabilized with Foxp3 fixation buffer (eBioscience) and stained with the following Abs: Helios (BioLegend, 22F6), Foxp3 (eBioscience, FJK-16s), GZMA (eBioscience, GzA-3G8.5), and granzyme B (Life Technologies, GB11). Stained cells were analyzed on a LSRFortessa II, and data were interpreted with FlowJo software. A fixable yellow dead cell stain kit (Life Technologies) was used to eliminate dead cells.

### Transcriptome analysis

Whole-genome expression was studied in iIEL  $\gamma\delta$  T cells and three different subsets of  $\gamma\delta$  T cells (T1, type naive-like, and T17) that are present in LNs. RNA was extracted in triplicates of each condition and hybridized into expression microarrays (GeneChip 2.0 ST from Affymetrix). The resulting CEL files were imported using the oligo package (18), and all downstream analyses were performed using this and other R/Bioconductor packages, R version 4.1.2 (2021-11-01) (<https://cran.r-project.org/>; <http://www.bioconductor.org/>). The robust multichip average algorithm from the oligo package was used for normalization, followed by inspection using principal component analysis (PCA) with ggplot2 functions (19). Differential expression was performed using limma functions to fit a linear model and contrasts for all pairwise comparisons (20). Significant probes (false discovery rate-adjusted  $p < 0.05$ ) were annotated with the annotation `mogene20stranscriptcluster.db` package (21) and visualized with EnhancedVolcano for volcano plots (22), eulerr for genelist overlaps (23), and NMF for annotated supervised and unsupervised heatmaps (24). Gene set enrichment analyses were performed using function from the packages clusterprofiler (25, 26), enrichplot (27), DOSE (28), ReactomePA (29), msigdb (30), and fgsea (31).

All code is available in GitHub ([https://github.com/hernandezvargash/iIEL\\_transcriptome.git](https://github.com/hernandezvargash/iIEL_transcriptome.git)), and all sequencing data have been uploaded into the Gene Expression Omnibus repository under accession number GSE198703 (<https://www.ncbi.nlm.nih.gov/geo/query/acc.cgi?acc=GSE198703>).

### Gene and pathway analysis

Gene enrichment analysis was performed with the Enrichr online tool (32). A STRING online algorithm was used to identify protein-protein interaction networks and to perform functional enrichment analysis (33).

### Statistical analysis

An unpaired Student  $t$  test was used to calculate statistical significance, defined as  $p < 0.05$ .

## RESULTS

### Distinct expression of CD44 and CD27 between iIEL $\gamma\delta$ T cells and other $\gamma\delta$ T cells

Given that CD27 and CD44 surface expression is classically used to discriminate T1 cells producing IFN- $\gamma$  (CD44<sup>+</sup>CD27<sup>+</sup>) and T17 cells (CD44<sup>high</sup>CD27<sup>-</sup>) producing IL-17 (12), we analyzed the expression of these markers on iIEL  $\gamma\delta$  T cells. This combination of markers enabled us to identify in the pLNs and skin the classically described T1 and T17 cells as well as the CD44<sup>low/-</sup>CD27<sup>+</sup>  $\gamma\delta$  T cells, recently defined as “naive-like,” unpolarized  $\gamma\delta$  T cells (Tn) (16) (Fig. 1). Although the T17 subset constituted a significant amount of  $\gamma\delta$  T cells in the pLNs and skin (38.1 and 71.7% respectively), they were scarcely detectable in iIEL  $\gamma\delta$  T cells from the SI and colon. Conversely,

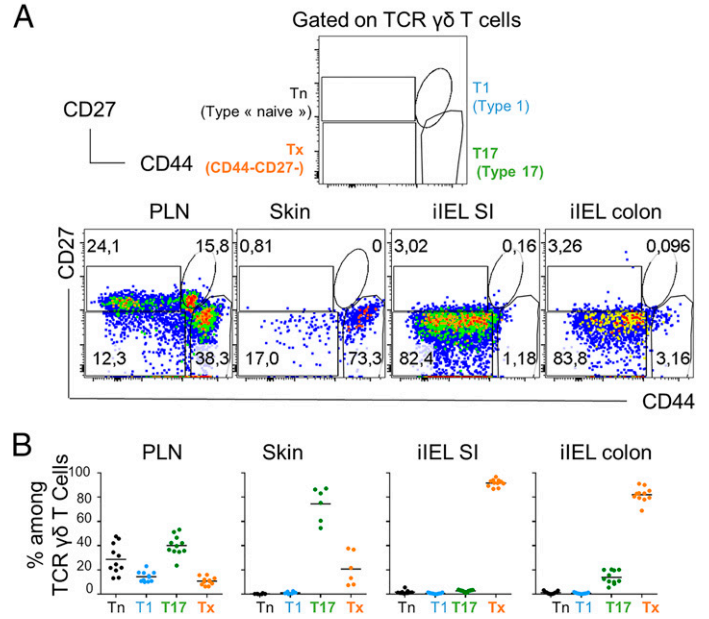


**FIGURE 1. Intestinal intraepithelial TCR  $\gamma\delta$  T cells display distinct CD44 and CD27 expression compared with the peripheral  $\gamma\delta$  T cells.**

(A) Flow cytometry analysis gated on total CD45<sup>+</sup>CD3<sup>+</sup> $\gamma\delta$ <sup>+</sup> T cells from pLNs, skin, the epithelium of the small intestine (SI), and the colon from 6-wk-old mice. The upper row shows a schematic representation of gating strategy of T1, T17, and naive-like  $\gamma\delta$  T cells. The middle row shows a representative flow cytometry plot illustrating CD44 and CD27 expression. (B) Graphs indicate the percentage of T1 (CD44<sup>+</sup>CD27<sup>+</sup>) cells (blue), T17 (CD44<sup>+</sup>CD27<sup>-</sup>) cells (green), naive-like (black)  $\gamma\delta$  T (Tn) cells, and the CD44<sup>low</sup>CD27<sup>low</sup> subset (Tx) (orange) among total  $\gamma\delta$  T cells ( $n = 6;11$ ). All data are representative of three experiments.

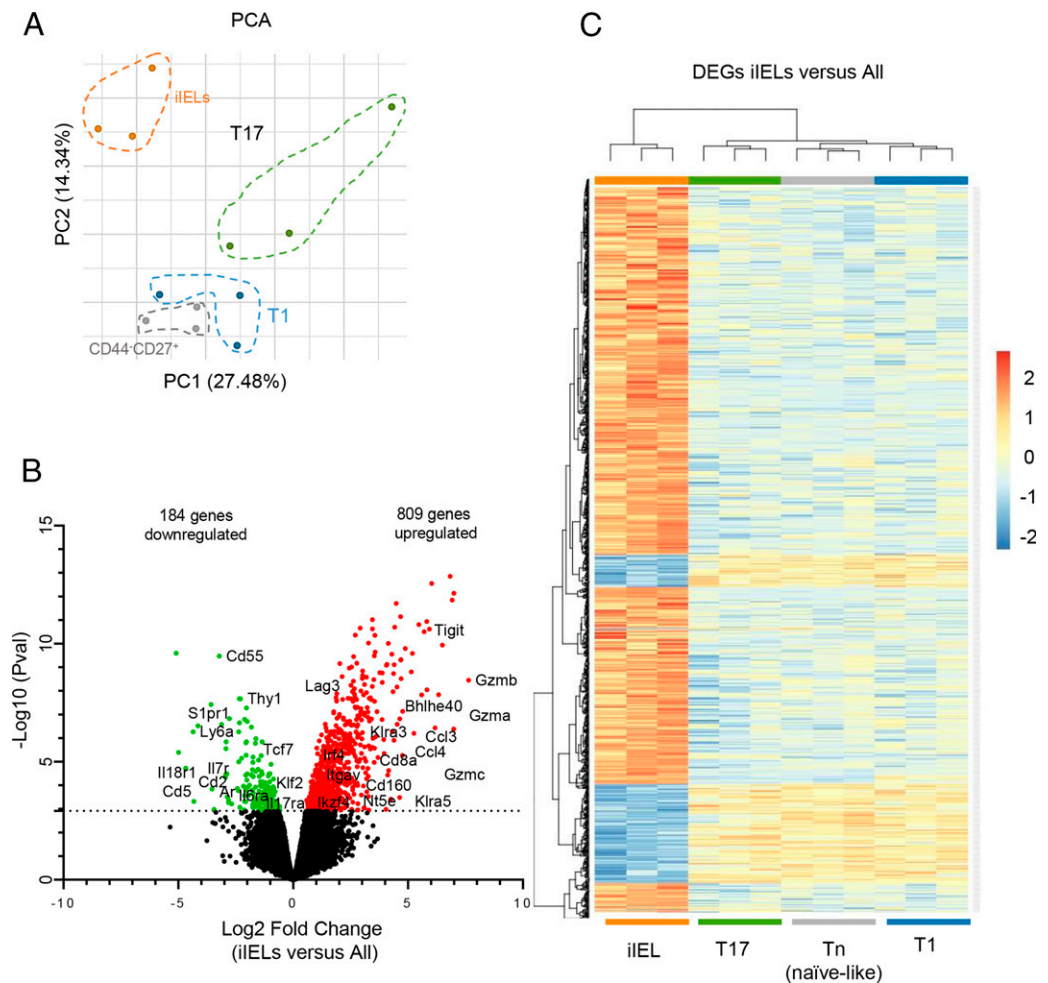
iIEL  $\gamma\delta$  T cells were predominantly represented by the CD44<sup>low/-</sup>CD27<sup>-</sup> population, which was barely detectable in the pLNs and skin (Fig. 1). These results define iIEL  $\gamma\delta$  T cells as a population with a different expression of CD44 and CD27 compared with their peripheral counterparts.

### Distinct gene expression between iIEL $\gamma\delta$ T cells and other $\gamma\delta$ T cells

To further compare iIEL  $\gamma\delta$  T cells with other subsets of TCR  $\gamma\delta$  T cells, we performed a wide transcriptomic analysis on FACS-sorted T1, T17, and Tn cells from pLNs and iIELs based on the expression of CD27 and CD44 markers (Fig. 2). First, to determine how the different subsets segregate and relate to each other, we conducted PCA. According to the PCA, the Tn fraction was transcriptionally very similar and closer to the T1 population than T17 cells. In clear contrast, the iIEL  $\gamma\delta$  T population appeared to be very distinct from the other subsets, even from Tn cells, to which they seemed closer based on CD44 and CD27 expression (Fig. 2A). Nine hundred ninety-three genes were differentially expressed in iIEL  $\gamma\delta$  T cells compared with the other  $\gamma\delta$  T cell types (Fig. 2B, Supplemental Fig. 1A) ( $p < 0.001$ , false discover rate 1%

**FIGURE 2. Intestinal intraepithelial TCR  $\gamma\delta$  T cells display a distinct gene expression profile compared with the peripheral  $\gamma\delta$  T cells.**

(A) Principal component analysis (PCA) based on transcriptome data was performed on naive-like, T17, and T1  $\gamma\delta$  T cells from pLNs and  $\gamma\delta$  T cells from intestinal epithelium from the small intestine. (B) Volcano plot graph of genes upregulated or downregulated in iIEL  $\gamma\delta$  T cells versus the other subsets. Highlighted in red is any gene with a  $p$  value  $<1e-05$  and  $\log_2$  fold change  $>0.5$  (upregulated in iIELs) or highlighted in green (less than  $-0.5$ ; downregulated in iIELs). (C) Hierarchical clustering of all differentially expressed genes (DEGs) ( $n = 993$ ).



with 95% confidence). Among these genes, 809 genes were upregulated and 184 were downregulated (Fig. 2C, Supplemental Fig. 1B). Hence, gene expression analysis confirmed that iIEL  $\gamma\delta$  T cells compose a distinct  $\gamma\delta$  T cell subset.

### **iIEL $\gamma\delta$ T cells are endowed with specific functionality**

To further characterize the iIEL  $\gamma\delta$  T cells, we conducted a functional analysis of the genes that differentiate them from the other subsets of  $\gamma\delta$  T cells. We used the Enrichr gene enrichment analysis tool (32) to extract transcripts expressed in the given cell types. In contrast to the other subsets, iIEL  $\gamma\delta$  T cells were enriched in transcripts of genes associated with cytotoxicity classically expressed in NK and cytotoxic CD8 T cells at steady-state conditions (Fig. 3A, 3B). This included *Gzmb*, *Gzma*, and *Gzmk* (Fig. 3A, Supplemental Fig. 1). The iIEL  $\gamma\delta$  T cells also strongly expressed the T1 cytokine IFN- $\gamma$  conjointly with T1  $\gamma\delta$  T cells (Fig. 3A). Confirming the cytotoxicity function at steady-state conditions, *Gzma* and *Gzmb* were expressed only by iIEL  $\gamma\delta$  T cells (Fig. 3C). Moreover, 2B4 (CD244), a non-MHC binding receptor previously reported as being expressed on cytotoxic lymphocytes such as CD8<sup>+</sup> T cells and NK cells (34), marked iIEL  $\gamma\delta$  T cells (Fig. 3C). iIEL  $\gamma\delta$  T cells expressed a specific cytokine and chemokine ligand signature including *Il18*, *Ccl3*, and *Ccl4*.

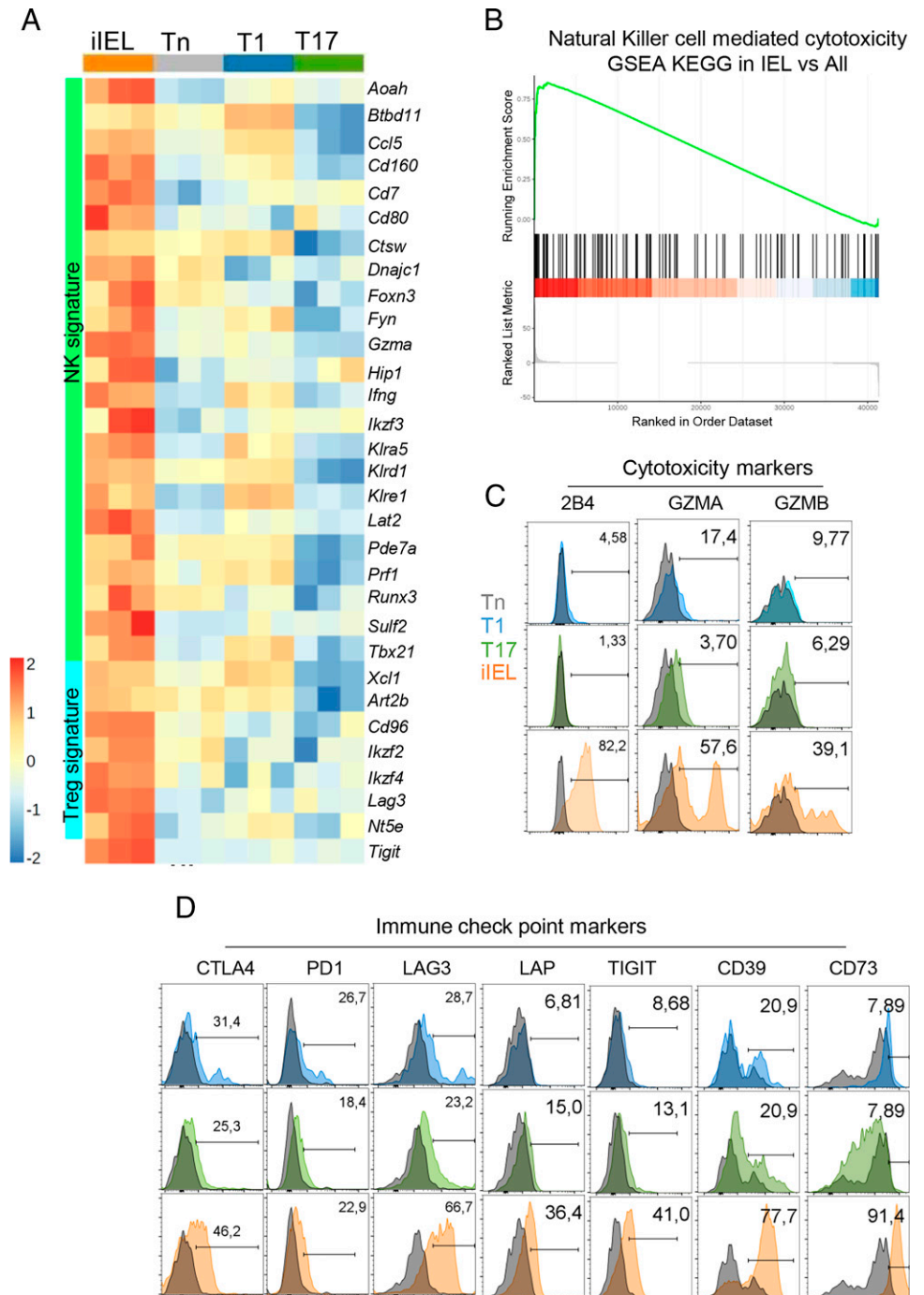
Interestingly, aside from their cytotoxic activity, iIEL  $\gamma\delta$  T cells selectively expressed genes linked to immunoregulatory function such as *Xcl1*, *Lag3*, *Tigit*, and *Nt5e* (Fig. 3A, Supplemental Fig. 1). Then, we sought to confirm at the protein level the expression of genes, reminiscent of the canonical Foxp3<sup>+</sup> regulatory T cells (Tregs). In iIEL  $\gamma\delta$  T cells, CD73 and CD39, two ectonucleotidases that generate extracellular adenosine by ATP hydrolysis and thus establish an immunosuppressive environment (35), were highly expressed when compared with the other subsets (Fig. 3D). The membrane-bound TGF- $\beta$ 1 through its accessory binding part LAP previously described on Tregs was also expressed at the surface of iIEL  $\gamma\delta$  T cells (Fig. 3D). As part of their immunoregulatory function, we found that iIEL  $\gamma\delta$  T cells also expressed coinhibitory receptors involved in immunosuppression, including *Lag3*, *TIGIT*, and *CTLA-4* (Fig. 3D). Overall, our data reveal that iIEL  $\gamma\delta$  T cells are endowed with distinct functionality compared with the other subsets of TCR  $\gamma\delta$  T cells, exhibiting both potent multi-effector functions and immunoregulatory features.

### **Combination of chemokine receptors to define $\gamma\delta$ T cell subsets**

Given that the aforementioned data suggest that iIEL  $\gamma\delta$  T cells compose a subset with specific functionality and that CD44

**FIGURE 3. Intestinal intraepithelial TCR  $\gamma\delta$  cells exhibit a dual cytotoxic–regulatory phenotype.**

(A) Heatmap representing clusters of genes with cytotoxic (green cluster) and regulatory (cyan cluster) functions differentially expressed between iIEL and peripheral  $\gamma\delta$  T cells (fold change > 2). Brown and blue indicate high and low expression, respectively. (B) Gene set enrichment analysis on differentially expressed genes of iIELs versus all. The plot shows enrichment of NK cell-mediated cytotoxicity signature in iIELs compared with all TCR  $\gamma\delta$  T cell subsets. (C) Representative flow cytometry histograms of 2B4, GZA, GZB, and FASL cytotoxic mediators in T1 (blue), T17 (green), and iIELs (orange) versus naive-like  $\gamma\delta$  T cells (Tn; gray) ( $n = 6$ ). (D) Flow cytometry analysis of regulatory marker expression: CTLA4, PD-1, LAG3, LAP, TIGIT, CD39, and CD73 in T1, T17, and iIEL  $\gamma\delta$  T cells compared with the control naive-like  $\gamma\delta$  T cells.

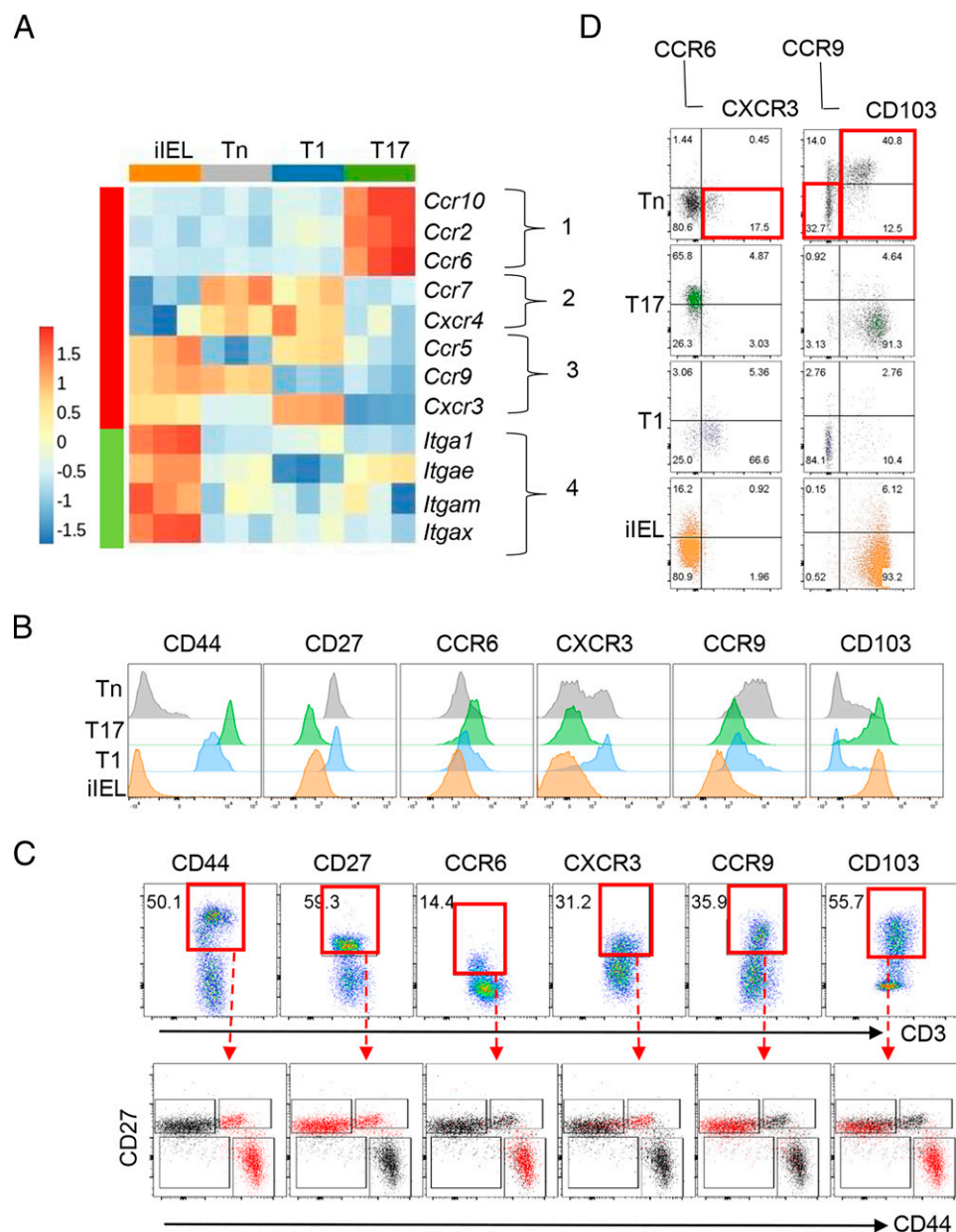


and CD27 expression is not the most efficient combination to distinguish them, we next tried to define surface markers specifically characterizing the iIEL  $\gamma\delta$  T fraction. To this end, we sorted the list of differentially expressed genes for several chemokine receptors and adhesion molecules in  $\gamma\delta$  T cell subsets. Four clusters were distinguished (Fig. 4A). Cluster 1 corresponds to chemokine receptor genes that appeared to be specific to T17 cells, including *Ccr6*, *Ccr2*, and *Ccr10*. In cluster 2, *Ccr7* and *Cxcr4* exclusively identified Tn and T1 cells. Although similar at transcriptional

levels (Fig. 2), Tn and T1 cells expressed some chemokine receptors that could help to further distinguish them. For instance, *Ccr9* was expressed by both Tn and iIEL  $\gamma\delta$  T cells, whereas *Ccr5* and *Cxcr3* were expressed by T1 and iIEL  $\gamma\delta$  T cells (cluster 3). Notably, none of the chemokine receptors was exclusively detected on iIEL  $\gamma\delta$  T cells. However, iIEL  $\gamma\delta$  T cells expressed the highest levels of adhesion molecules and integrins such as *Itga1*, *Itgae*, *Itgam*, and *Itgax* (CD11c) that specifically identify them (cluster 4) (Fig. 4A). Cytometry staining further demonstrated

**FIGURE 4. Intestinal intraepithelial TCR  $\gamma\delta$  T cells express different sets of chemokine receptors et adhesion molecules.**

(A) Heatmap representing clusters of chemokine receptors (red cluster) and adhesion molecules (green cluster) differentially expressed between iIEL and peripheral  $\gamma\delta$  T cells (fold change > 2). Brown and blue indicate high and low expression, respectively. (B) Representative flow cytometry histograms of the indicated markers in Tn (gray), T17 (green), T1 (blue), and iIELs (orange)  $\gamma\delta$  T cell populations. (C) Representative flow cytometry histograms of the indicated markers in total  $\gamma\delta$  T cells from the peripheral lymph nodes. (D) Representative flow cytometry histograms of the indicated markers in the different peripheral  $\gamma\delta$  T cell fractions from the peripheral lymph nodes versus iIELs. All data are representative of two experiments ( $n = 8$ ).



that the expression of chemokine receptors could be used to better characterize the different subsets of TCR  $\gamma\delta$  T cells (Fig. 4B, 4C). Of note, *Itgae* that encodes for CD103 involved in epithelial retention (36) was also remarkably expressed by T17  $\gamma\delta$  T cells and thus could not be used to separate T17 from iIEL  $\gamma\delta$  T cells (Fig. 4C, 4D). However, in pLNs, high levels of expression of the CD103 marker allowed us to distinguish T17 TCR  $\gamma\delta$  T cells. It is noteworthy that the iIEL TCR  $\gamma\delta$  T cells express CD69 and CD49a markers associated with tissue residency (37), which suggests that they are closely related to resident T cells (Supplemental Fig. 2). Unexpectedly, the cytometry analysis uncovered that the Tn subset was not a homogeneous population. Indeed, based on CD103 and CXCR3, we observed three Tn

populations. The first one displayed markers similar to those expressed by iIEL  $\gamma\delta$  T cells and T17 (CD103) cells, the second one to T1 (CXCR3) cells, and the third one expressed none of the markers associated with iIEL, T1, or T17 cells, likely representing the bona fide unpolarized TCR  $\gamma\delta$  T cell population (Fig. 4D). Interestingly, the cytometry analysis confirmed the unique expression of CCR9 in Tn cells and a small fraction of iIEL populations, thereby distinguishing them from all the other subtypes (Fig. 4D). Overall, our data indicate new cell surface markers that can be employed in addition to the currently used ones (CD44 and CD27) to better differentiate the TCR  $\gamma\delta$  T cell subsets.

#### Transcription factors define $\gamma\delta$ T cell subsets

The transcriptome analysis clearly demonstrated the presence of transcription factors specific for each  $\gamma\delta$  T cell subtype



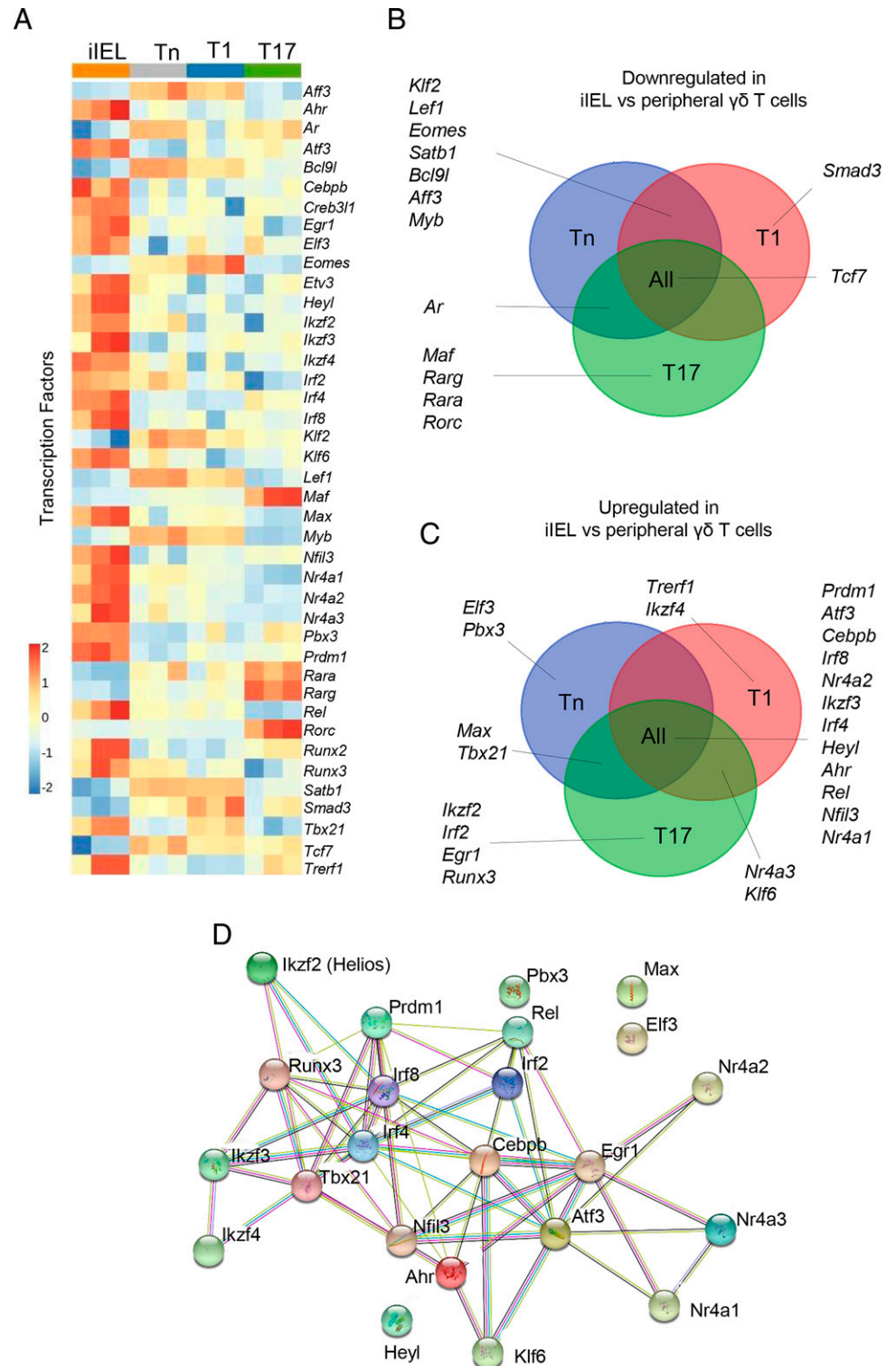


**FIGURE 5. Unique network of transcription factors distinguishes the peripheral and the intestinal intraepithelial TCR  $\gamma\delta$  T cell fractions.**

(A) Heatmap indicating the transcription factors differentially expressed between iIEL and peripheral  $\gamma\delta$  T cells (fold change > 2). Brown and blue indicate high and low expression, respectively. (B and C) Schematic representation of the transcription factors either downregulated (B) or upregulated (C) in the iIEL versus the peripheral TCR  $\gamma\delta$  T cell fractions. (D) Interaction enrichment map of transcription factors upregulated in the iIEL versus the peripheral TCR  $\gamma\delta$  T fractions (protein–protein interaction enrichment  $p$  value <  $1.0e-16$ ) generated with the STRING protein–protein association network algorithm.

(Fig. 5A). *Rorc*, *Maf*, *Rora*, and *Rarg* high expression was characteristic of the T17 population whereas *Tcf7* selectively downregulated the iIEL  $\gamma\delta$  T cell population (Fig. 5A, 5B). Next, we sought to analyze the transcription factors characteristic of iIEL  $\gamma\delta$  T cells. Of note, numerous transcription factors were upregulated in the iIEL  $\gamma\delta$  T cells when compared with all of

the peripheral  $\gamma\delta$  T cell fractions (Fig. 5A, 5C). Five of the 12 transcription factors upregulated in iIEL  $\gamma\delta$  T cells have been associated with Treg homeostasis maintenance, differentiation, as well as immune tolerance: *Ahr* (38–41), *Blimp-1* (42–44), *Irf4* (45, 46), *Nfil3* (47, 48), and *Nr4a* (49–51). In particular, two of these transcription factors, *Blimp-1* and *Irf4*, have been

reported to jointly control the differentiation and function of effector Tregs (52). In addition, among the upregulated genes encoding for transcriptional factors, Helios (*Irf2*) was largely specific to iIEL  $\gamma\delta$  T cells (Fig. 5A), previously implicated in the maintenance of the immunosuppressive function of Tregs (53). Although iIEL  $\gamma\delta$  T cells represented common features with Tregs (Supplemental Fig. 3A), they did not express Foxp3 (Supplemental Fig. 3B). We next analyzed whether the iIEL  $\gamma\delta$  T cell-specific transcription factors may form a functional network. We used the STRING algorithm to identify protein-protein interaction networks and to perform functional enrichment analysis (33). The interaction enrichment map (protein-protein interaction enrichment  $p < 1.0e-16$ ) of the transcription factors upregulated in iIELs  $\gamma\delta$  T cells versus all their counterparts suggests that most of them form a functionally connected network (Fig. 5D). Altogether, these results suggest that the iIEL  $\gamma\delta$  T cells can be defined by the expression of transcription factors that could work in concert to establish a unique transcriptional program.

#### **A marked Helios expression distinguishes $\gamma\delta$ TCR or $\alpha\beta$ TCR natural iIELs versus induced iIELs**

As iIEL  $\gamma\delta$  T cells of the intestine express a high level of Helios, we wondered whether this expression was specific to the cell localization in the intestine epithelium. Therefore, we analyzed by flow cytometry the expression of the Helios transcription factor in  $\gamma\delta$  T cells in different organs. Among the analyzed organs (liver, spleen, LNs, skin, thymus), we observed a strong expression of Helios within the  $\gamma\delta$  T cells present within the intestine, in particular within the epithelium as compared with those present in the lamina propria (Fig. 6A–C). Thus, we investigated whether the expression of Helios is a unique characteristic of iIEL  $\gamma\delta$  T cells or could be a common feature shared with other subsets of iIELs. Strikingly, the expression of Helios was predominantly restrained to natural iIEL  $\gamma\delta$  T cells and TCR $\alpha\beta$ CD8 $\alpha\alpha$  T cells. Indeed, CD4<sup>+</sup>CD8 $\alpha\alpha$  TCR $\alpha\beta$  T cells and CD8 $\alpha\beta$  TCR $\alpha\beta$  T cells failed to express Helios. Even though we could detect a small population of Helios-positive cells among the conventional CD8 $\alpha\beta$  TCR $\alpha\beta$  T cells, we observed that Helios expression differentiates the induced  $\alpha\beta$ TCR CD4<sup>+</sup>CD8 $\alpha\alpha$  versus the natural CD8 $\alpha\alpha$  T cells (Fig. 6D, 6E). In the intestine, the high expression of Helios was restricted to natural iIEL T cells because the induced iIELs also present in the epithelium poorly express Helios. Thus, this data set implies Helios expression as a hallmark of natural iIEL T cells irrelevant to TCR $\alpha\beta$  or TCR $\gamma\delta$  expression.

#### **Intestinal epithelium cues and modulation by TGF- $\beta$ signaling drive Helios expression in natural iIELs**

The accumulation of Helios-expressing iIEL cells suggests that a factor of the intestine microenvironment may favor its expression. We ruled out the contribution of the microbiota because treatment with a large spectrum of antibiotics since in utero life did not affect Helios expression in iIEL T cells (Fig. 7A–C). Given that TGF- $\beta$  signaling is important for the maintenance of Helios

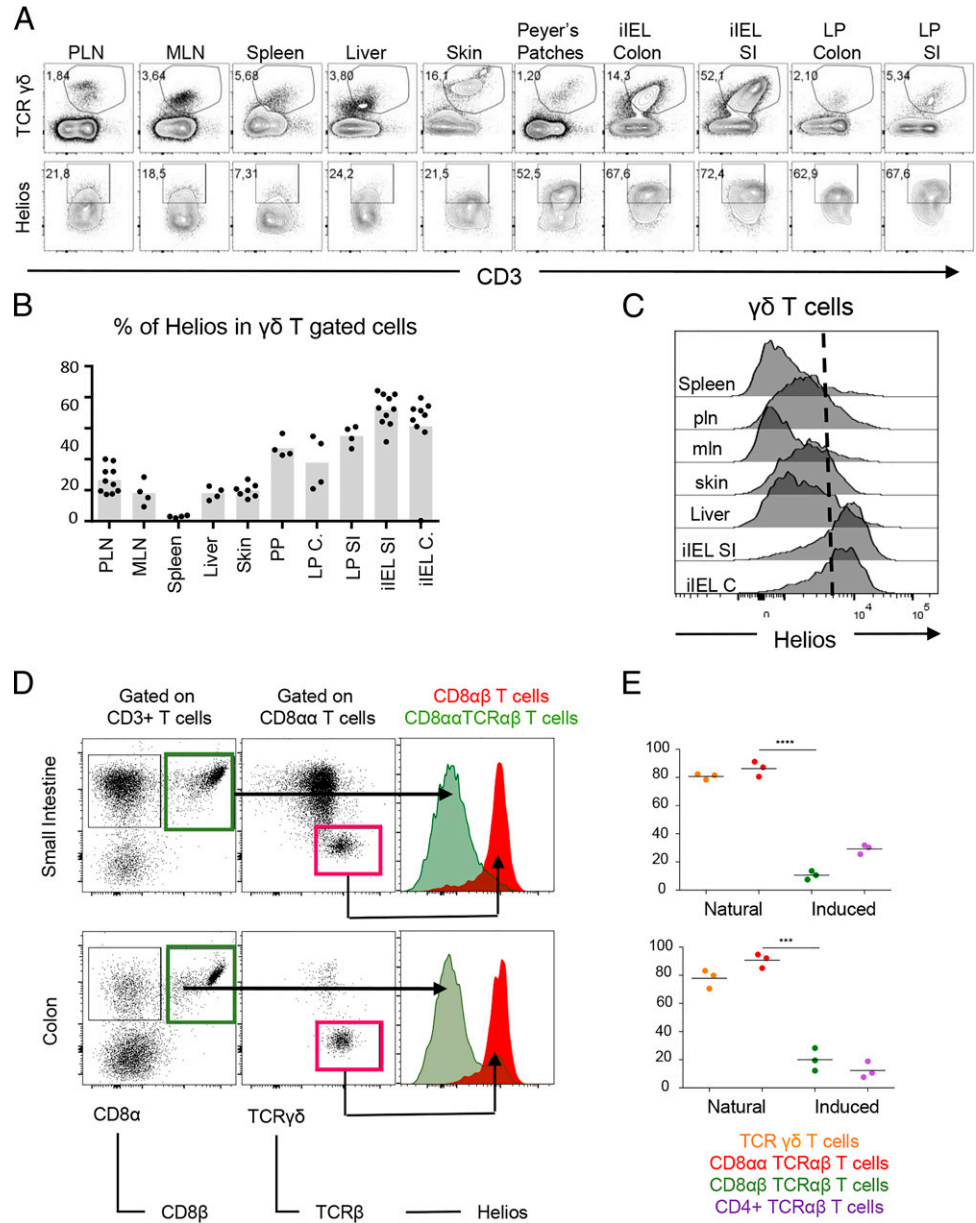
expression and the regulatory identity of the CD4<sup>+</sup> Treg subset as well as the CD8<sup>+</sup> Tregs (54) and that the intestine contains high levels of TGF- $\beta$  (55), we then investigated whether TGF- $\beta$  signaling can regulate Helios expression in the iIEL T cells. CD4-Cre;Tgfb $\beta$ 2<sup>fl/fl</sup> mice (Fig. 7D), targeting *tgfb2* expression selectively on  $\alpha\beta$  T cells and not on  $\gamma\delta$  T cells, (56, 57) revealed a 2-fold decrease of Helios expression in the natural CD8 $\alpha\alpha$  TCR $\alpha\beta$  T cells but not TCR  $\gamma\delta$  T cells in the SI and colon (Fig. 7D). Hence, TGF- $\beta$  signaling contributes to high Helios expression in the natural intraepithelial T lymphocytes.

## **DISCUSSION**

In the current study, we compare intestinal  $\gamma\delta$  T cells with  $\gamma\delta$  T cell subsets found in other tissues. iIEL  $\gamma\delta$  T cells are a particular subset of lymphocytes based on their phenotype and their function. Several studies have done a comparison of the  $\gamma\delta$  T cells of the intestine with bulk  $\gamma\delta$  T cells or with  $\alpha\beta$  T cells present in pLNs (13, 14). The goal of our study is the comparison of three different subsets of  $\gamma\delta$  T cells identified by the expression of CD27 and CD44 markers that discriminate distinct known subsets of  $\gamma\delta$  T cells in the periphery. Interestingly, our data show that the iIEL  $\gamma\delta$  T cells are CD44<sup>low</sup>CD27<sup>-</sup>, demarcating them from T1 (CD44<sup>+</sup>CD27<sup>+</sup>), T17 (CD44<sup>+</sup>CD27<sup>-</sup>), or the naive-like type (CD44<sup>low/-</sup>CD27<sup>+</sup>)  $\gamma\delta$  T cells present in the periphery. This phenotype was unexpected because iIEL  $\gamma\delta$  T cells are described as experienced T cells, and the low CD44 expression is therefore not common. The whole transcriptome analysis supported that iIEL  $\gamma\delta$  T cells are a distinct group compared with the lymph node  $\gamma\delta$  T subsets, based on the differential expression of adhesion molecules, chemokine receptors, and transcription factors. Seeking a transcription factor that might dictate the peculiar cytotoxic regulatory functional phenotype, we focused on Helios, which has been reported to maintain the stability of Foxp3<sup>+</sup> Tregs (53, 58). We have shown that the expression of Helios seems to be independent of Foxp3 expression, in contrast to Tregs, where its expression has been mostly reported to be associated with and to be a way to define the thymic-derived Tregs (53). However, its independence with Foxp3 expression suggests it may perform other functions in iIEL  $\gamma\delta$  T cells compared with the classic Tregs. Previous studies have also shown that the Helios expression could be associated with an activated stage of T cells (59). This double capacity of Helios could be due to the activation of different pathways and genes leading to T cell regulation and functional cytotoxicity. Chromatin immunoprecipitation sequencing could be realized, permitting the definition of Helios-targeted genes in  $\gamma\delta$  T cells. We can hypothesize that the transcription factor Helios could be a key factor explaining the specific phenotype of  $\gamma\delta$  T cells in the intestinal epithelium. However, the redundancy with the other members of the family of Helios, such as Ikaros, Aiolos, or Eos, could compensate for the lack of Helios, a speculation that has to be formally proven. Indeed, Helios knockout in mice did not significantly affect T cell development (60) even in Tregs, suggesting a compensatory role

**FIGURE 6. Helios expression predominantly marks the iIEL T cells.**

(A) Representative flow cytometry plot of cells harvested from different tissues (pLNs, mesenteric lymph nodes [MLNs], spleen, liver, skin, Peyer’s patches, intestinal epithelium of colon [C] and small intestine [SI], and lamina propria of colon and SI). The upper row depicts the gating strategy on  $\gamma\delta$  T cells, and the lower row depicts the expression of Helios in  $\gamma\delta$  T cells. (B and C) Histograms of the percentage of Helios-expressing cells (B) and mean fluorescence intensity of Helios expression (C) in  $\gamma\delta$  T cells from each tissue. (D) FACS plots representing the gating strategy on CD8 $\alpha\alpha$ TCR $\alpha\beta$  (red) and CD8 $\alpha\beta$  T cells (green) and the expression of Helios in CD8 $\alpha\alpha$  (red) and CD8 $\alpha\beta$  (green) T cells within the epithelium of the SI. (E) Histogram representing the percentage of Helios-expressing cells among the “natural” and the “induced” iIELs.  $\gamma\delta$  T cells (orange), CD8 $\alpha\alpha$  TCR $\alpha\beta$  cells (red), CD8 $\alpha\beta$  TCR $\alpha\beta$  cells (green), and CD4 TCR $\alpha\beta$  cells (purple). All data are representative of two experiments. \*\*\* $p < 0.001$ , \*\*\*\* $p < 0.0001$ , by two-tailed Student *t* test.



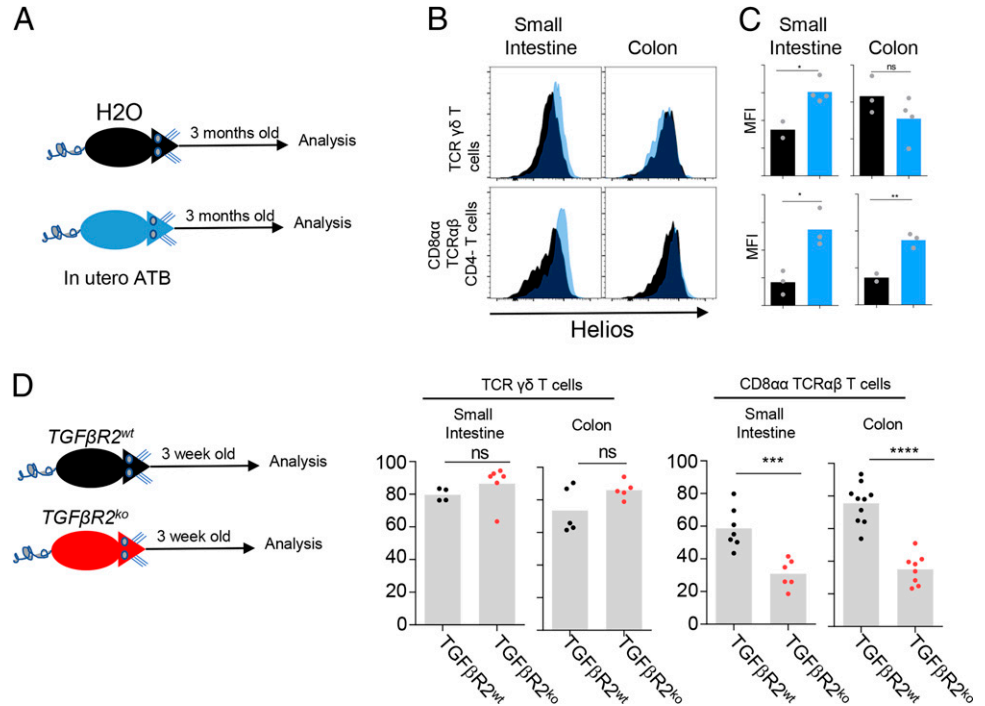
of other Ikaros family members. In addition, our data highlight the high expression of Helios as a marker that could delineate unconventional iIELs to induced iIEL  $\alpha\beta$  T cells. Indeed, in mice, Helios expression demarcates the natural iIEL  $\gamma\delta$  T and CD8 $\alpha\alpha$   $\alpha\beta$  T cells from the induced CD8 $\alpha\beta$   $\alpha\beta$  T cells, at least at a steady state.

Several studies have suggested that both CD8 $\alpha\alpha$  TCR $\alpha\beta$  and TCR $\gamma\delta$  iIELs manifest regulatory phenotype (61–63). Our transcriptome and flow cytometry analyses have confirmed the expression of genes with effector functions and suggested that iIEL  $\gamma\delta$  T cells share important features with regulatory cells through the expression of additional genes with regulatory functions, such as TIGIT, CD39, CD73, LAP, Lag-3, CTLA-4, PD-1, Helios, and Eos in the absence of the Foxp3 transcription factor.

Additionally, this particular phenotype of iIEL  $\gamma\delta$  T cells and CD8 $\alpha\alpha$   $\alpha\beta$  T cells within the intestine raises the important question of the role of the gut environment in establishing this characteristic. Our first assumption was that microbiota present in abundance within the intestine could trigger the expression of Helios within the unconventional iIELs. However, we failed to demonstrate the implication of the microbiota by analyzing mice treated with an antibiotic in utero, a result favoring a self-antigen-driven Helios expression. Thus, other intestinal cues could mediate the upregulation of Helios in natural iIELs. The lack of expression of Helios by the innate iIELs that do not harbor a TCR may suggest that a signal coming for the TCR is involved. Within the intestine, some abundantly expressed cytokines, such as TGF- $\beta$ , may contribute to the establishment of intestinal

**FIGURE 7. Helios expression is not induced by intestinal microbiota but is driven by intestinal epithelium cues and modulated by TGF- $\beta$  signaling.**

(A) Mice were put on water or antibiotic (ATB)-treated water in utero and left on antibiotics until 3 mo old. (B) Representative FACS showing Helios expression in the indicated populations on ATB-treated mice (blue) or not treated ones (black). (C) Histogram showing mean fluorescence intensity (MFI) of Helios expression on  $\gamma\delta$  T cells from mice water treated (black) and ATB-treated ones (blue). (D) Percentage of Helios expression in  $\gamma\delta$  T cells and CD8 $\alpha\alpha$  TCR $\alpha\beta$  T cells from TGF- $\beta$ 2<sup>w<sup>t</sup></sup> (wild-type) or TGF- $\beta$ 2<sup>ko</sup> (knockout) mice. All data are representative of two experiments. \**p* < 0.05, \*\**p* < 0.01, \*\*\**p* < 0.001, \*\*\*\**p* < 0.0001, by two-tailed Student *t* test; ns, not significant.



homeostasis. Hence, it will be interesting to address the role of TGF- $\beta$  signaling on Helios expression specifically in unconventional iIELs by appropriate genetic models. In the current study, we do not have a genetic model to delete the TGF- $\beta$  receptor specifically in TCR  $\gamma\delta$  or CD8 $\alpha\alpha$   $\alpha\beta$  T iIELs without affecting the induced ones. Using the CD4-driven Cre system, we could only address the impact of TGF- $\beta$  signaling on Helios expression in natural CD8 $\alpha\alpha$  TCR $\alpha\beta$  iIELs, which allowed us to demonstrate that TGF- $\beta$  signaling within the intestine promotes Helios expression.

We cannot rule out that Helios expression in iIELs and probably their “regulatory-like” features might be related to aspects such as the origin and specifics of their TCR signaling. Several studies have revealed that CD8 $\alpha\alpha$  TCR $\alpha\beta$  iIEL development can occur both extrathymically (64–66) and from thymic iIEL precursors (67–71). It has also been proposed that strong agonist selection in thymocytes correlates with the expression of genes, such as Helios, Nur77, Bim, and PD-1 in thymocytes (72–77) and that CD8 $\alpha\alpha$  TCR $\alpha\beta$  cells can originate from self-reactive double-positive thymocytes (78). These cells can also be selected on MHC class I- or class II-restricted agonist self-peptides (68) and nonconventional MHC class I-related chain A (MICA) molecules expressed in the intestinal epithelium (79, 80). All of these data, taken together with the observation that Helios expression is detected in thymic iIEL precursors (81, 82), suggest that genes enriched in the  $\gamma\delta$  T iIELs, such as Helios, Bim, Nur77, and PD-1, might be induced by strong, self-driven, and constant TCR stimulation in the periphery, where their potential inducers might be the expression of self-molecules, such as butyrophilins (*Btn1* and *Btn6*) produced by the intestinal epithelium (8).

In summary, we have provided more novel evidence that iIEL  $\gamma\delta$  T cells are a peculiar cell type expressing a unique group of transcription factors, which functionally separates them from the peripheral subsets of  $\gamma\delta$  T cells. They do not exhibit a T17 or T1 profile and may be considered as an immunoregulatory subset with effector functions characterized by the expression of Helios, a transcription factor, which could be used as a surrogate marker to define the unconventional iIELs.

## DISCLOSURES

The authors have no financial conflicts of interest.

## ACKNOWLEDGMENTS

We thank all the past and present members of the Marie laboratory for help and discussions. We thank the platforms of the CRCL, including the flow cytometry, genomic, as well as the animal facility (Anican/P-PAC), for advice, help, and assistance.

## REFERENCES

1. Vancamelbeke, M., and S. Vermeire. 2017. The intestinal barrier: a fundamental role in health and disease. *Expert Rev. Gastroenterol. Hepatol.* 11: 821–834.
2. Larsen, S. B., C. J. Cowley, and E. Fuchs. 2020. Epithelial cells: liaisons of immunity. *Curr. Opin. Immunol.* 62: 45–53.
3. Peterson, L. W., and D. Artis. 2014. Intestinal epithelial cells: regulators of barrier function and immune homeostasis. *Nat. Rev. Immunol.* 14: 141–153.

4. Olivares-Villagómez, D., and L. Van Kaer. 2018. Intestinal intraepithelial lymphocytes: sentinels of the mucosal barrier. *Trends Immunol.* 39: 264–275.
5. Cheroutre, H., F. Lambolez, and D. Mucida. 2011. The light and dark sides of intestinal intraepithelial lymphocytes. *Nat. Rev. Immunol.* 11: 445–456.
6. Uehara, S., A. Grinberg, J. M. Farber, and P. E. Love. 2002. A role for CCR9 in T lymphocyte development and migration. *J. Immunol.* 168: 2811–2819.
7. Barbee, S. D., M. J. Woodward, G. Turchinovich, J.-J. Mention, J. M. Lewis, L. M. Boyden, R. P. Lifton, R. Tigelaar, and A. C. Hayday. 2011. Skint-1 is a highly specific, unique selecting component for epidermal T cells. *Proc. Natl. Acad. Sci. USA* 108: 3330–3335.
8. Di Marco Barros, R., N. A. Roberts, R. J. Dart, P. Vantourout, A. Jandke, O. Nussbaumer, L. Deban, S. Cipolat, R. Hart, M. L. Iannitto, et al. 2016. Epithelia use butyrophilin-like molecules to shape organ-specific  $\gamma\delta$  T cell compartments. *Cell* 167: 203–218.e17.
9. Chennupati, V., T. Worbs, X. Liu, F. H. Malinarich, S. Schmitz, J. D. Haas, B. Malissen, R. Förster, and I. Prinz. 2010. Intra- and inter-compartmental movement of  $\gamma\delta$  T cells: intestinal intraepithelial and peripheral  $\gamma\delta$  T cells represent exclusive nonoverlapping populations with distinct migration characteristics. *J. Immunol.* 185: 5160–5168.
10. Chen, Y., K. Chou, E. Fuchs, W. L. Havran, and R. Boismenu. 2002. Protection of the intestinal mucosa by intraepithelial  $\gamma\delta$  T cells. *Proc. Natl. Acad. Sci. USA* 99: 14338–14343.
11. Ismail, A. S., C. L. Behrendt, and L. V. Hooper. 2009. Reciprocal interactions between commensal bacteria and  $\gamma\delta$  intraepithelial lymphocytes during mucosal injury. *J. Immunol.* 182: 3047–3054.
12. Ribot, J. C., A. deBarros, D. J. Pang, J. F. Neves, V. Peperzak, S. J. Roberts, M. Girardi, J. Borst, A. C. Hayday, D. J. Pennington, and B. Silva-Santos. 2009. CD27 is a thymic determinant of the balance between interferon- $\gamma$ - and interleukin 17-producing  $\gamma\delta$  T cell subsets. *Nat. Immunol.* 10: 427–436.
13. Hedges, J. F., J. C. Graff, and M. A. Jutila. 2003. Transcriptional profiling of  $\gamma\delta$  T cells. *J. Immunol.* 171: 4959–4964.
14. Shires, J., E. Theodoridis, and A. C. Hayday. 2001. Biological insights into TCR $\gamma\delta^+$  and TCR $\alpha\beta^+$  intraepithelial lymphocytes provided by serial analysis of gene expression (SAGE). *Immunity* 15: 419–434.
15. Fahrner, A. M., Y. Konigshofer, E. M. Kerr, G. Ghandour, D. H. Mack, M. M. Davis, and Y. H. Chien. 2001. Attributes of  $\gamma\delta$  intraepithelial lymphocytes as suggested by their transcriptional profile. *Proc. Natl. Acad. Sci. USA* 98: 10261–10266.
16. Sagar, M. Pokrovskii, J. S. Herman, S. Naik, E. Sock, P. Zeis, U. Lausch, M. Wegner, Y. Tanriver, D. R. Littman, and D. Grün. 2020. Deciphering the regulatory landscape of fetal and adult  $\gamma\delta$  T-cell development at single-cell resolution. *EMBO J.* 39: e104159.
17. Igalouzene, R., H. Hernandez-Vargas, N. Benech, A. Guyennon, D. Bauché, C. Barrachina, E. Dubois, J. C. Marie, and S. M. Soudja. 2022. SMAD4 TGF- $\beta$ -independent function preconditions naive CD8 $^+$  T cells to prevent severe chronic intestinal inflammation. *J. Clin. Invest.* 132: e151020.
18. Carvalho, B. S., and R. A. Irizarry. 2010. A framework for oligonucleotide microarray preprocessing. *Bioinformatics* 26: 2363–2367.
19. Wickham, H. 2016. *ggplot2: Elegant Graphics for Data Analysis*. Springer, New York.
20. Ritchie, M. E., B. Phipson, D. Wu, Y. Hu, C. W. Law, W. Shi, and G. K. Smyth. 2015. limma powers differential expression analysis for RNA-sequencing and microarray studies. *Nucleic Acids Res.* 43: e47.
21. MacDonald, J.W. 2017. mogene20stranscriptcluster.db: Affymetrix mogene20 annotation data (chip mogene20stranscriptcluster). R package version 8.7.0. Available at: <https://bioconductor.org/packages/release/data/annotation/html/mogene20stranscriptcluster.db.html>.
22. Blighe, K., S. Rana, and M. Lewis. 2022. EnhancedVolcano: publication-ready volcano plots with enhanced colouring and labeling. R package version 1.14.0. Available at: <https://github.com/kevinblighe/EnhancedVolcano>.
23. Larsson, J., and P. Gustafsson. 2018. A case study in fitting area-proportional euler diagrams with ellipses using eulerr. In 6th International Workshop on Set Visualization and Reasoning, SetVR 2018. *CEUR Workshop Proc.* 2116: 84–91. Available at: <http://ceur-ws.org/Vol-2116/paper7.pdf>.
24. Gaujoux, R., and C. Seoighe. 2010. A flexible R package for nonnegative matrix factorization. *BMC Bioinformatics* 11: 367.
25. Wu, T., E. Hu, S. Xu, M. Chen, P. Guo, Z. Dai, T. Feng, L. Zhou, W. Tang, L. Zhan, et al. 2021. clusterProfiler 4.0: a universal enrichment tool for interpreting omics data. *Innovation (Camb)* 2: 100141.
26. Yu, G., L.-G. Wang, Y. Han, and Q.-Y. He. 2012. clusterProfiler: an R package for comparing biological themes among gene clusters. *OMICS* 16: 284–287.
27. Yu, G. 2022. enrichplot: visualization of functional enrichment result. R package version 1.16.1. Available at: <https://yulab-smu.top/biomedical-knowledge-mining-book/>.
28. Yu, G., L.-G. Wang, G.-R. Yan, and Q.-Y. He. 2015. DOSE: an R/Bioconductor package for disease ontology semantic and enrichment analysis. *Bioinformatics* 31: 608–609.
29. Yu, G., and Q.-Y. He. 2016. ReactomePA: an R/Bioconductor package for reactome pathway analysis and visualization. *Mol. Biosyst.* 12: 477–479.
30. Dolgalev, I. 2021. igordot/msigdb: msigdb 7.4.1. Zenodo. Available at: <https://github.com/igordot/msigdb/releases/tag/v7.4.1>.
31. G. Korotkevich, V. Sukhov, and A. Sergushichev. 2019. Fast gene set enrichment analysis. Available at: <https://bioconductor.org/packages/release/bioc/html/fgsea.html>.
32. Chen, E. Y., C. M. Tan, Y. Kou, Q. Duan, Z. Wang, G. V. Meirelles, N. R. Clark, and A. Ma'ayan. 2013. Enrichr: interactive and collaborative HTML5 gene list enrichment analysis tool. *BMC Bioinformatics* 14: 128.
33. Szklarczyk, D., A. L. Gable, K. C. Nastou, D. Lyon, R. Kirsch, S. Pyysalo, N. T. Doncheva, M. Legeay, T. Fang, P. Bork, et al. 2021. The STRING database in 2021: customizable protein-protein networks, and functional characterization of user-uploaded gene/measurements sets. *Nucleic Acids Res.* 49(D1): D605–D612.
34. Rey, J., J. Giustiniani, F. Mallet, V. Schiavon, L. Boumsell, A. Bensussan, D. Olive, and R. T. Costello. 2006. The co-expression of 2B4 (CD244) and CD160 delineates a subpopulation of human CD8 $^+$  T cells with a potent CD160-mediated cytolytic effector function. *Eur. J. Immunol.* 36: 2359–2366.
35. Bono, M. R., D. Fernández, F. Flores-Santibáñez, M. Roseblatt, and D. Sauma. 2015. CD73 and CD39 ectonucleotidases in T cell differentiation: Beyond immunosuppression. *FEBS Lett.* 589: 3454–3460.
36. Do, J., S. Kim, K. Keslar, E. Jang, E. Huang, R. L. Fairchild, T. T. Pizarro, and B. Min. 2017.  $\gamma\delta$  T cells coexpressing gut homing  $\alpha 4\beta 7$  and  $\alpha E$  integrins define a novel subset promoting intestinal inflammation. *J. Immunol.* 198: 908–915.
37. Park, S. L., T. Gebhardt, and L. K. Mackay. 2019. Tissue-resident memory T cells in cancer immunosurveillance. *Trends Immunol.* 40: 735–747.
38. Funatake, C. J., N. B. Marshall, L. B. Steppan, D. V. Mourich, and N. I. Kerkvliet. 2005. Cutting edge: activation of the aryl hydrocarbon receptor by 2,3,7,8-tetrachlorodibenzo-p-dioxin generates a population of CD4 $^+$ CD25 $^+$  cells with characteristics of regulatory T cells. *J. Immunol.* 175: 4184–4188.
39. Kerkvliet, N. I. 2009. AHR-mediated immunomodulation: the role of altered gene transcription. *Biochem. Pharmacol.* 77: 746–760.
40. Mezrich, J. D., J. H. Fechner, X. Zhang, B. P. Johnson, W. J. Burlingham, and C. A. Bradfield. 2010. An interaction between

- kyurenine and the aryl hydrocarbon receptor can generate regulatory T cells. *J. Immunol.* 185: 3190–3198.
41. Singh, N. P., U. P. Singh, B. Singh, R. L. Price, M. Nagarkatti, and P. S. Nagarkatti. 2011. Activation of aryl hydrocarbon receptor (AhR) leads to reciprocal epigenetic regulation of FoxP3 and IL-17 expression and amelioration of experimental colitis. *PLoS One* 6: e23522.
  42. Lin, M.-H., F.-C. Chou, L.-T. Yeh, S.-H. Fu, H.-Y. C. Chiou, K.-I. Lin, D.-M. Chang, and H.-K. Sytwu. 2013. B lymphocyte-induced maturation protein 1 (BLIMP-1) attenuates autoimmune diabetes in NOD mice by suppressing Th1 and Th17 cells. *Diabetologia* 56: 136–146.
  43. Cretney, E., P. S. K. Leung, S. Trezise, D. M. Newman, L. C. Rankin, C. E. Teh, T. L. Putoczki, D. H. D. Gray, G. T. Belz, L. A. Mielke, et al. 2018. Characterization of Blimp-1 function in effector regulatory T cells. *J. Autoimmun.* 91: 73–82.
  44. Ogawa, C., R. Bankoti, T. Nguyen, N. Hassanzadeh-Kiabi, S. Nadeau, R. A. Porritt, M. Couse, X. Fan, D. Dhall, G. Eberl, et al. 2018. Blimp-1 functions as a molecular switch to prevent inflammatory activity in Foxp3<sup>+</sup>ROR $\gamma$ t<sup>+</sup> regulatory T cells. *Cell Rep.* 25: 19–28.e5.
  45. Zheng, Y., A. Chaudhry, A. Kas, P. deRoos, J. M. Kim, T.-T. Chu, L. Corcoran, P. Treuting, U. Klein, and A. Y. Rudensky. 2009. Regulatory T-cell suppressor program co-opts transcription factor IRF4 to control T<sub>H</sub>2 responses. *Nature* 458: 351–356.
  46. Alvisi, G., J. Brummelman, S. Puccio, E. M. C. Mazza, E. P. Tomada, A. Losurdo, V. Zanon, C. Peano, F. S. Colombo, A. Scarpa, et al. 2020. IRF4 instructs effector Treg differentiation and immune suppression in human cancer. *J. Clin. Invest.* 130: 3137–3150.
  47. Motomura, Y., H. Kitamura, A. Hijikata, Y. Matsunaga, K. Matsumoto, H. Inoue, K. Atarashi, S. Hori, H. Watarai, J. Zhu, et al. 2011. The transcription factor E4BP4 regulates the production of IL-10 and IL-13 in CD4<sup>+</sup> T cells. *Nat. Immunol.* 12: 450–459.
  48. Zhu, C., K. Sakuishi, S. Xiao, Z. Sun, S. Zaghouni, G. Gu, C. Wang, D. J. Tan, C. Wu, M. Rangachari, et al. 2015. An IL-27/NFIL3 signaling axis drives Tim-3 and IL-10 expression and T-cell dysfunction. [Published erratum appears in 2015 *Nat. Commun.* 6: 7657.] *Nat. Commun.* 6: 6072.
  49. Sekiya, T., I. Kashiwagi, N. Inoue, R. Morita, S. Hori, H. Waldmann, A. Y. Rudensky, H. Ichinose, D. Metzger, P. Chambon, and A. Yoshimura. 2011. The nuclear orphan receptor Nr4a2 induces Foxp3 and regulates differentiation of CD4<sup>+</sup> T cells. *Nat. Commun.* 2: 269.
  50. Sekiya, T., T. Kondo, T. Shichita, R. Morita, H. Ichinose, and A. Yoshimura. 2015. Suppression of Th2 and Tfh immune reactions by Nr4a receptors in mature T reg cells. *J. Exp. Med.* 212: 1623–1640.
  51. Sekiya, T., S. Kagawa, K. Masaki, K. Fukunaga, A. Yoshimura, and S. Takaki. 2021. Regulation of peripheral Th/Treg differentiation and suppression of airway inflammation by Nr4a transcription factors. *iScience* 24: 102166.
  52. Cretney, E., A. Xin, W. Shi, M. Minnich, F. Masson, M. Miasari, G. T. Belz, G. K. Smyth, M. Busslinger, S. L. Nutt, and A. Kallies. 2011. The transcription factors Blimp-1 and IRF4 jointly control the differentiation and function of effector regulatory T cells. *Nat. Immunol.* 12: 304–311.
  53. Kim, H.-J., R. A. Barnitz, T. Kreslavsky, F. D. Brown, H. Moffett, M. E. Lemieux, Y. Kaygusuz, T. Meissner, T. A. W. Holderried, S. Chan, et al. 2015. Stable inhibitory activity of regulatory T cells requires the transcription factor Helios. *Science* 350: 334–339.
  54. Mishra, S., W. Liao, Y. Liu, M. Yang, C. Ma, H. Wu, M. Zhao, X. Zhang, Y. Qiu, Q. Lu, and N. Zhang. 2021. TGF- $\beta$  and Eomes control the homeostasis of CD8<sup>+</sup> regulatory T cells. *J. Exp. Med.* 218: e20200030.
  55. Bauché, D., and J. C. Marie. 2017. Transforming growth factor  $\beta$ : a master regulator of the gut microbiota and immune cell interactions. *Clin. Transl. Immunology* 6: e136.
  56. Dudley, E. C., H. T. Petrie, L. M. Shah, M. J. Owen, and A. C. Hayday. 1994. T cell receptor  $\beta$  chain gene rearrangement and selection during thymocyte development in adult mice. *Immunity* 1: 83–93.
  57. Taghon, T., M. A. Yui, R. Pant, R. A. Diamond, and E. V. Rothenberg. 2006. Developmental and molecular characterization of emerging  $\beta$ - and  $\gamma\delta$ -selected pre-T cells in the adult mouse thymus. *Immunity* 24: 53–64.
  58. Sebastian, M., M. Lopez-Ocasio, A. Metidji, S. A. Rieder, E. M. Shevach, and A. M. Thornton. 2016. Helios controls a limited subset of regulatory T cell functions. *J. Immunol.* 196: 144–155.
  59. Akimova, T., U. H. Beier, L. Wang, M. H. Levine, and W. W. Hancock. 2011. Helios expression is a marker of T cell activation and proliferation. *PLoS One* 6: e24226.
  60. Cai, Q., A. Dierich, M. Oulad-Abdelghani, S. Chan, and P. Kastner. 2009. Helios deficiency has minimal impact on T cell development and function. *J. Immunol.* 183: 2303–2311.
  61. Denning, T. L., S. W. Granger, S. Granger, D. Mucida, R. Graddy, G. Leclercq, W. Zhang, K. Honey, J. P. Rasmussen, H. Cheroutre, et al. 2007. Mouse TCR $\alpha\beta$ <sup>+</sup>CD8 $\alpha\alpha$  intraepithelial lymphocytes express genes that down-regulate their antigen reactivity and suppress immune responses. *J. Immunol.* 178: 4230–4239.
  62. Poussier, P., T. Ning, D. Banerjee, and M. Julius. 2002. A unique subset of self-specific intraintestinal T cells maintains gut integrity. *J. Exp. Med.* 195: 1491–1497.
  63. Kamanaka, M., S. T. Kim, Y. Y. Wan, F. S. Sutterwala, M. Lara-Tejero, J. E. Galán, E. Harhaj, and R. A. Flavell. 2006. Expression of interleukin-10 in intestinal lymphocytes detected by an interleukin-10 reporter knockin tiger mouse. *Immunity* 25: 941–952.
  64. Kanamori, Y., K. Ishimaru, M. Nanno, K. Maki, K. Ikuta, H. Nariuchi, and H. Ishikawa. 1996. Identification of novel lymphoid tissues in murine intestinal mucosa where clusters of c-kit<sup>+</sup> IL-7R<sup>+</sup> Thy1<sup>+</sup> lymphohemopoietic progenitors develop. *J. Exp. Med.* 184: 1449–1459.
  65. Saito, H., Y. Kanamori, T. Takemori, H. Nariuchi, E. Kubota, H. Takahashi-Iwanaga, T. Iwanaga, and H. Ishikawa. 1998. Generation of intestinal T cells from progenitors residing in gut cryptopatches. *Science* 280: 275–278.
  66. Suzuki, K., T. Oida, H. Hamada, O. Hitotsumatsu, M. Watanabe, T. Hibi, H. Yamamoto, E. Kubota, S. Kaminogawa, and H. Ishikawa. 2000. Gut cryptopatches: direct evidence of extrathymic anatomical sites for intestinal T lymphopoiesis. *Immunity* 13: 691–702.
  67. Lefrançois, L., and S. Olson. 1994. A novel pathway of thymus-directed T lymphocyte maturation. *J. Immunol.* 153: 987–995.
  68. Leishman, A. J., L. Gapin, M. Capone, E. Palmer, H. R. MacDonald, M. Kronenberg, and H. Cheroutre. 2002. Precursors of functional MHC class I- or class II-restricted CD8 $\alpha\alpha$ <sup>+</sup> T cells are positively selected in the thymus by agonist self-peptides. *Immunity* 16: 355–364.
  69. Guy-Grand, D., O. Azogui, S. Celli, S. Darche, M. C. Nussenzweig, P. Kourilsky, and P. Vassalli. 2003. Extrathymic T cell lymphopoiesis: ontogeny and contribution to gut intraepithelial lymphocytes in athymic and euthymic mice. *J. Exp. Med.* 197: 333–341.
  70. Eberl, G., and D. R. Littman. 2004. Thymic origin of intestinal  $\alpha\beta$  T cells revealed by fate mapping of ROR $\gamma$ t<sup>+</sup> cells. *Science* 305: 248–251.
  71. Ruscher, R., R. L. Kummer, Y. J. Lee, S. C. Jameson, and K. A. Hogquist. 2017. CD8 $\alpha\alpha$  intraepithelial lymphocytes arise from two main thymic precursors. *Nat. Immunol.* 18: 771–779.
  72. Mingueneau, M., T. Kreslavsky, D. Gray, T. Heng, R. Cruse, J. Ericson, S. Bendall, M. H. Spitzer, G. P. Nolan, K. Kobayashi, et al.; Immunological Genome Consortium. 2013. The transcriptional landscape of  $\alpha\beta$  T cell differentiation. *Nat. Immunol.* 14: 619–632.
  73. Marsden, V. S., and A. Strasser. 2003. Control of apoptosis in the immune system: Bcl-2, BH3-only proteins and more. *Annu. Rev. Immunol.* 21: 71–105.
  74. Baldwin, T. A., and K. A. Hogquist. 2007. Transcriptional analysis of clonal deletion in vivo. *J. Immunol.* 179: 837–844.
  75. Bouillet, P., J. F. Purton, D. I. Godfrey, L.-C. Zhang, L. Coultas, H. Puthalakath, M. Pellegrini, S. Cory, J. M. Adams, and A. Strasser. 2002. BH3-only Bcl-2 family member Bim is required for apoptosis

- of autoreactive thymocytes. [Published erratum appears in 2002 *Nature* 418: 108.] *Nature* 415: 922–926.
76. Daley, S. R., D. Y. Hu, and C. C. Goodnow. 2013. Helios marks strongly autoreactive CD4<sup>+</sup> T cells in two major waves of thymic deletion distinguished by induction of PD-1 or NF- $\kappa$ B. *J. Exp. Med.* 210: 269–285.
  77. Stritesky, G. L., Y. Xing, J. R. Erickson, L. A. Kalekar, X. Wang, D. L. Mueller, S. C. Jameson, and K. A. Hogquist. 2013. Murine thymic selection quantified using a unique method to capture deleted T cells. *Proc. Natl. Acad. Sci. USA* 110: 4679–4684.
  78. Yamagata, T., D. Mathis, and C. Benoist. 2004. Self-reactivity in thymic double-positive cells commits cells to a CD8 $\alpha\alpha$  lineage with characteristics of innate immune cells. *Nat. Immunol.* 5: 597–605.
  79. Leishman, A. J., O. V. Naidenko, A. Attinger, F. Koning, C. J. Lena, Y. Xiong, H.-C. Chang, E. Reinherz, M. Kronenberg, and H. Cheroutre. 2001. T cell responses modulated through interaction between CD8 $\alpha\alpha$  and the nonclassical MHC class I molecule, TL. *Science* 294: 1936–1939.
  80. Park, E. J., I. Takahashi, J. Ikeda, K. Kawahara, T. Okamoto, M.-N. Kweon, S. Fukuyama, V. Groh, T. Spies, Y. Obata, et al. 2003. Clonal expansion of double-positive intraepithelial lymphocytes by MHC class I-related chain A expressed in mouse small intestinal epithelium. *J. Immunol.* 171: 4131–4139.
  81. Klose, C. S. N., K. Blatz, Y. d'Hargues, P. P. Hernandez, M. Kofoed-Nielsen, J. F. Ripka, K. Ebert, S. J. Arnold, A. Diefenbach, E. Palmer, and Y. Tanriver. 2014. The transcription factor T-bet is induced by IL-15 and thymic agonist selection and controls CD8 $\alpha\alpha$ <sup>+</sup> intraepithelial lymphocyte development. *Immunity* 41: 230–243.
  82. Hummel, J. F., P. Zeis, K. Ebert, J. Fixemer, P. Konrad, C. Schachtrup, S. J. Arnold, D. Grün, and Y. Tanriver. 2020. Single-cell RNA-sequencing identifies the developmental trajectory of C-Myc-dependent NK1.1<sup>−</sup> T-bet<sup>+</sup> intraepithelial lymphocyte precursors. *Mucosal Immunol.* 13: 257–270.